

Small Graph Is All You Need: DeepStateGNN for Scalable Traffic Forecasting

Yannick Wölker^{1*}, Arash Hajisafi^{2*}, Cyrus Shahabi², Matthias Renz¹

¹Department of Computer Science, Kiel University, Kiel, Germany
{ywoe, mr}@informatik.uni-kiel.de

²Department of Computer Science, University of Southern California, Los Angeles, USA
{hajisafi, shahabi}@usc.edu

Abstract

We propose a novel Graph Neural Network (GNN) model, named DeepStateGNN, for analyzing traffic data, demonstrating its efficacy in two critical tasks: forecasting and reconstruction. Unlike typical GNN methods that treat each traffic sensor as an individual graph node, DeepStateGNN clusters sensors into higher-level graph nodes, dubbed Deep State Nodes, based on various similarity criteria, resulting in a fixed number of nodes in a Deep State graph. The term “Deep State” nodes is a play on words, referencing hidden networks of power that, like these nodes, secretly govern traffic independently of visible sensors. These Deep State Nodes are defined by several similarity factors, including spatial proximity (e.g., sensors located nearby in the road network), functional similarity (e.g., sensors on similar types of freeways), and behavioral similarity under specific conditions (e.g., traffic behavior during rain). This clustering approach allows for dynamic and adaptive node grouping, as sensors can belong to multiple clusters and clusters may evolve over time. Our experimental results show that DeepStateGNN offers superior scalability and faster training, while also delivering more accurate results than competitors. It effectively handles large-scale sensor networks, outperforming other methods in both traffic forecasting and reconstruction accuracy.

1 Introduction

Traffic flow forecasting is a critical function in spatiotemporal forecasting research, providing insights to guide infrastructure development, enhance safety, improve traffic management, and integrate multimodal transportation systems. Presently, traffic data is collected either through loop-detector sensors installed on roads or through trajectory data from vehicles, which is often transformed into traffic flow at discrete points along the road, effectively creating virtual sensors¹ (Li et al. 2020). Regardless of the acquisition method, this aggregated traffic data forms time series, making traffic forecasting a multivariate time-series forecasting task.

This spatiotemporal forecasting task is challenging due to complex spatiotemporal dependencies across sensors and issues with long-term dependencies in the sensors themselves.

*These authors contributed equally.

¹Hereafter, the term “sensor” will refer to both real and virtual sensors.

Previous studies have shown that graphs are effective in capturing these complex relationships (Li et al. 2018), leading to the use of graph-based approaches for traffic forecasting. These approaches model inter-sensor dependencies as a sensor graph, capturing relationships through message-passing techniques. However, there are shortcomings, three of which we highlight here.

First, as the number of sensors increases to cover larger areas, the sensor graph grows so large that memory and computation requirements become infeasible. Consequently, these approaches are typically applied to datasets containing only highway sensors, excluding smaller arterial roads, which are crucial for analyzing traffic flow.

Second, these approaches rely on a static set of sensors and require continuous data from all sensors, making them inflexible when sensors are added, removed, or experience failures. In production environments, traffic sensors can experience outages, leading to missing data. Prominent benchmark datasets like METR-LA and PEMS-BAY (Li et al. 2018) preprocess their data to include only sensors that are consistently available. Some studies explore imputation as a method to fill these gaps, where missing sensor data is treated similarly to traffic prediction. However, these methods are brittle with respect to the sensor network and struggle with long-term changes in sensor layouts. When cities update their sensor layouts or add new streets with sensors, even imputation-based techniques require retraining and expanding the sensor graph.

Third, most previous GNN-based approaches focus on a single type of road, typically highways, when modeling traffic. However, different road types exhibit different traffic patterns. For example, highways show strong traffic signal propagation along their length (Pan et al. 2022), resulting in strong auto-correlations. In contrast, urban arterial roads exhibit more diverse traffic patterns. Shao et al. (Shao et al. 2022) highlight the importance of modeling different road classes for effective traffic forecasting, but prior work has often neglected this due to the reliance on benchmark datasets that contain only highway data.

To tackle these shortcomings, our core idea is to group similar sensors for a more effective and reliable representation instead of using a traditional sensor graph with one node for each sensor. However, such an aggregated view often leads to information loss, and how to group sensors effec-

tively remains a challenge. These groupings should be dynamic and non-exclusive, as sensor similarities change depending on time and context. For example, sensors in different parts of a city may show similar patterns during rainy rush hours but differ on sunny holiday afternoons. Learning to group sensors and represent each sensor through a combination of observed traffic patterns from such groups can provide a fixed-size representation that scales easily and handles changes in sensor availability.

Consequently, we introduce the DeepState Graph Neural Network (DeepStateGNN) framework, which utilizes a fixed-size graph, called the DeepState graph. In this graph, each node, dubbed a DeepState Node (DSN), represents groups of sensors rather than individual sensors. These groupings are dynamically formed based on external factors such as spatial location, time, environmental conditions, or the similarity of traffic patterns captured by sensors. Each DSN aggregates the information from its corresponding sensor group into a latent state. The term “Deep State” is a playful nod to the concept of hidden networks of influence, mirroring how these nodes covertly form powerful clusters that govern the state of traffic independently of the individual sensor nodes, much like a “deep state” in political discourse operates behind the scenes.

The relationships between DSNs, both long-term and short-term, are represented as edges in the DeepState graph. A message-passing operation on the DeepState graph allows DSNs to exchange information about the traffic state with other related DSNs. Intuitively, this decomposition allows each DSN to specialize in representing specific traffic patterns, like traffic during rainy days or in particular neighborhoods. A traffic observation can be seen as a combination of these specialized nodes. Thus, this decomposition enables the inference of unknown traffic states at any location in the road network by querying a combination of DSN states that are semantically close to the query for the given time window.

Overall, our main contributions are as follows:

- We introduce DeepStateGNN, a novel framework that learns a fixed-size graph representation that captures the latent traffic state for groups of similar sensors during a time window. This graph can be queried to forecast or reconstruct traffic data for locations with missing or not yet observed sensors.
- Our approach, with a fixed number of high-level nodes in the graph representation, is flexible and can handle datasets where sensors are added, removed, or relocated. This adaptability allows for greater data utilization and reduces the need for frequent retraining in real-world applications.
- The proposed architecture outperforms all previous state-of-the-art baselines in both traffic forecasting and reconstruction accuracy, while also demonstrating superior computational scalability, achieving both without compromising one for the other.
- We propose and publish the METR-LA+ traffic dataset, sourced from the same data as METR-LA and PeMS-Bay (Li et al. 2018). This dataset provides an in-the-wild

representation of real-world traffic conditions compared to previous curated datasets. It includes two months of traffic data from both freeways and nearby arterial roads, incorporates missing sensors, and is enriched with additional information such as weather, air quality, and road semantics, for the same study area, tagged with location and time.

We validate our contributions through three stages of experiments. First, we show that DeepStateGNN outperforms state-of-the-art baselines on both freeway sensors and the broader network that includes arterial roads, with improvements ranging up to 40% across all metrics. We evaluate the generalization of our approach on two tasks: traffic prediction and reconstruction. Second, we demonstrate the scalability of DeepStateGNN, showing that our fixed-size graph representation results in better scaling of training times compared to those of the baselines. Finally, an ablation study validates the effectiveness of our DeepState nodes and the design choices regarding the graph-based representation.

2 Related Work

Traffic forecasting models often rely on data from static sensors, such as loop detectors or trajectory-based flows, which are geo-referenced and map-matched on the road network. This makes them well-suited for graph-based modeling. Early methods, such as STGCN (Yu, Yin, and Zhu 2018) and DCRNN (Li et al. 2018), used road network distances to construct static adjacency matrices. These static adjacency matrices capture street directionality but require many graph convolutional network (GCN) (Kipf and Welling 2017) steps to propagate across large network areas. To address the limitations of static adjacency matrices, (Wu et al. 2019) introduced Graph WaveNet, which employs a self-adaptive adjacency matrix optimized through stochastic gradient descent. This approach does not rely on prior road network information; instead, it uses static node embeddings, with the transition matrix formed by applying softmax to the product of these embeddings. A3T-GCN (Bai et al. 2021) leverages an attention mechanism to generate attention scores across different timestamps, while maintaining a static, binary adjacency matrix connecting direct neighbors. With the rise of graph attention mechanisms like GAT (Veličković et al. 2018), attention-based techniques were incorporated into spatiotemporal traffic forecasting. D2STGNN (Shao et al. 2022) utilizes this concept by creating dynamic transition matrices with a self-attention mechanism. It leverages historical traffic data, temporal context, and static node embeddings, similar to Graph WaveNet, to produce context-dependent transition matrices. Although this method is more dynamic, it is tied to a sensor graph. Moreover, all of these methods treated sensors as graph nodes, limiting their scalability and, as a result, focusing solely on a small, curated set of freeway sensors provided by previous studies.

Beyond traffic forecasting, only two recent studies have employed the concept of high-level graph nodes. The first, BysGNN (Hajisafi et al. 2023), predicts visitor numbers for Points of Interest (POIs) by modeling them as a graph with meta nodes representing clusters of similar POIs. The dy-

dynamic adjacency matrix is a function of spatial distance, temporal, and semantic embeddings. However, these meta nodes are manually crafted, static, and coexist with POIs in the graph, rather than fully representing them. The second work, SUSTeR (Wölker et al. 2023), uses a graph with only abstract nodes. The adjacency matrix is derived from node embeddings based on assigned sensors. However, SUSTeR employs a static, learned assignment from sensors to abstract nodes based solely on spatial features, without dynamic grouping. Therefore, the SUSTeR focused only on reconstruction and not forecasting. In Section 5, we compare DeepStateGNN with both BysGNN and SUSTeR.

3 Preliminaries

For traffic reconstruction and forecasting, we incorporated additional environmental, semantic, and positional factors as contextual data. Together, these factors create a comprehensive view of traffic dynamics.

Traffic Observation: A traffic observation consists of a combination of traffic measurements (including speed and flow) and contextual information at a specific sensor location during a defined time window.

Deep State Node (DSN): Traffic sensors that exhibit similar characteristics can be grouped and represented through Deep State Nodes (DSNs). In this work, we consider four DSN types: Spatial DSNs group sensors based on their geographical properties (e.g., neighborhood). Semantic DSNs cluster sensors according to road features (e.g., maximum lane speed). Environmental DSNs group sensors by similarity of weather and air quality conditions at their locations. Temporal DSNs cluster sensors based on observed traffic patterns.

Deep State Graph (DSG): A Deep State Graph is a compact, fixed-size graph representing the traffic network. Nodes in the DSG correspond to DSNs, each maintaining a latent state based on the aggregated observations of the sensors they represent. Edges in the DSG capture the short- and long-term similarities between these latent states.

Traffic Forecasting and Reconstruction Problems: Given a window k of traffic observations of length W , denoted as $X^{(k)} = (x_1^{(k)}, \dots, x_W^{(k)}) \in \mathbb{R}^{|S^{(k)}| \times W \times F}$, where each x_i^k represents a traffic observation with F features (traffic and contextual) for a subset of sensors $S^{(k)}$ in the road network, as well as a window of query observations $X_q^{(k)} = (x_{q_1}^{(k)}, \dots, x_{q_W}^{(k)}) \in \mathbb{R}^{|Q^{(k)}| \times W \times (F-2)}$ providing only the contextual values (missing speed and traffic flow measurements) for a query set of sensors $Q^{(k)}$ that don't overlap with S , the task is to:

(I) **Traffic Reconstruction:** Reconstruct the traffic measurements for the last $H \in \mathbb{N}^{\leq W}$ timestamps of the input window for the query set $Q^{(k)}$, represented as $\hat{Y}_{Reconstruct}^{(K)} = (\hat{y}_{W-H+1}, \dots, \hat{y}_W) \in \mathbb{R}^{|Q^{(k)}| \times H \times 2}$.

(II) **Traffic Forecasting:** Predict future traffic measurements over a horizon H for the query sensors $Q^{(k)}$ represented as $\hat{Y}_{Forecast}^{(K)} = (\hat{y}_{W+1}, \dots, \hat{y}_{W+H}) \in \mathbb{R}^{|Q^{(k)}| \times H \times 2}$.

To align with the goal of generalizing the traffic state for queries involving unknown sensors, we intentionally avoid

the simpler forecasting scenario, where the traffic values of the query sensors are part of the input. Instead, we present our forecasting approach (Definition II) as a more challenging and realistic problem setting. For simplicity of expressions, we drop the (k) superscript for the rest of the paper.

4 Proposed Model (DeepStateGNN)

DeepStateGNN addresses the scalability and flexibility challenges of previous GNN-based traffic forecasting and reconstruction methods. The architecture, shown in Figure 1, constructs a Deep State Graph (DSG) composed of a fixed number of Deep State Nodes (DSNs) representing sensor groups and their relationships. Graph Convolution is applied to the DSG to capture inter-node relationships in the DSN embeddings. These embeddings are then used to infer traffic conditions for query locations.

4.1 Deep State Graph Construction

The DSG represents the latent traffic state through DSNs that aggregate traffic observations from multiple sensors in a latent space. DSN states are initialized using an MLP based on the global input context, including the time of day and day of the week in our tasks. A combination of hand-crafted and learned metrics is employed to compute non-exclusive assignments from observations to DSNs. The rationale for using different types of assignments is that for some DSNs, such as spatial nodes, the assignment of sensors is straightforward based on spatial coverage. In contrast, the assignment for other DSNs, like environmental ones, is not predetermined and requires learning from data. After the assignment, the observations are embedded and aggregated to update the DSN states. Finally, the weighted and directional edges of the DSG are inferred based on long- and short-term relationships between DSN states. These steps are detailed in the following sections.

4.2 Observation Assignments

Static Assignments to Spatial and Semantic DSNs Observation assignments to spatial and semantic DSNs are static, as the spatial and semantic properties of each traffic sensor remain unchanged during the observed window. For spatial DSNs, one DSN is allocated per neighborhood and freeway. Assignments are based on the distance of the traffic sensor to the neighborhood center (soft assignment) or a binary assignment indicating whether the sensor is located on the specific road the DSN represents. For semantic DSNs, nodes are allocated for each semantic property, such as the number of lanes or maximum speed (e.g., one DSN for a max speed of 40 MPH). Observations are assigned to these nodes based on binary criteria reflecting the semantic properties of the road that the sensor that recorded the observation is placed on.

Dynamic Assignments to Environmental and Temporal DSNs DSG includes environmental and temporal DSNs that group traffic observations from sensors based on environmental factors (in our case weather and air quality) and temporal patterns. Sensors recording observations under similar conditions (e.g., same precipitation level) or showing

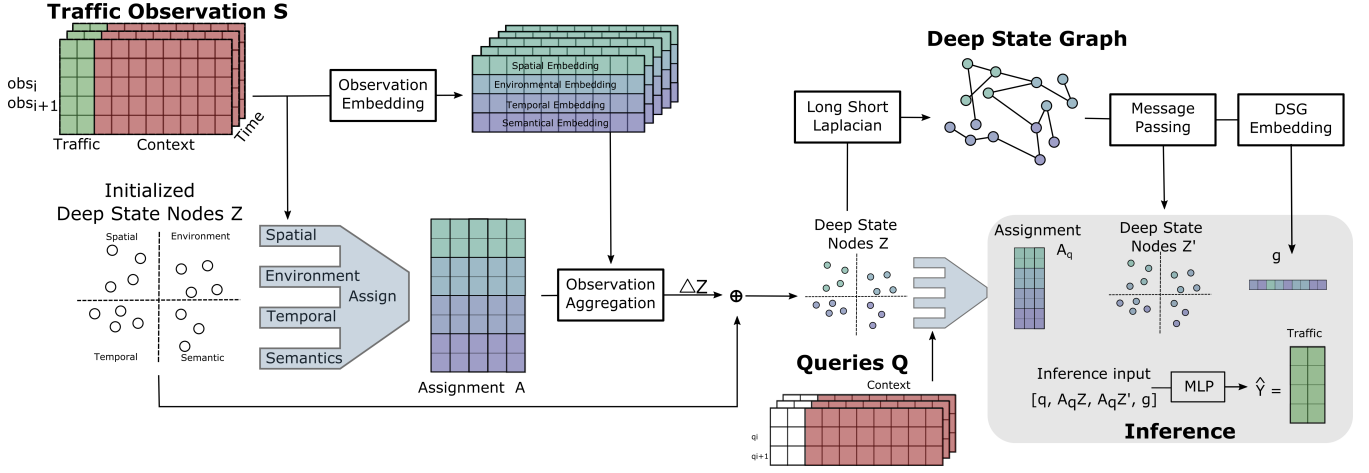


Figure 1: Overall DeepStateGNN Architecture.

similar traffic patterns should be mapped to the same environmental/temporal DSNs. Since the clusters corresponding to these DSNs (e.g., “rainy” environment) and the assignments from sensors to DSNs cannot be predefined, they must be learned from data. To achieve this, we specify the number of such DSNs as a hyperparameter and initialize their states using the same MLP as other DSNs.

The assignment process involves learning a gating-based mechanism, implemented as an MLP, that assigns soft weights from each observation to each DSN. For a given DSN type (denoted as Z_{type}), the input features X_f , relevant to that DSN type (e.g., all weather-related features for environmental DSNs), are used in the assignment. The assignment function is defined as follows:

$$a_i = gate([X_f; z_i]), \forall z_i \in Z_{type} \quad (1)$$

Here, z_i represents the state vector of a single DSN, and $[\cdot; \cdot]$ denotes the concatenation operation. Each observation in the set X_f is assigned an assignment vector $a_i \in \mathbb{R}^{|Z_{type}|}$. Concatenating all the assignment vectors forms the assignment matrix $A_{type} \in \mathbb{R}^{|Z_{type}| \times |S|}$ for the specific DSN type, where $|S|$ is the number of observation sensors.

After each DSN type generates its type-specific assignment matrix for both static and dynamic types, these partial matrices are concatenated into a single large matrix. The output of the assignment step is a tensor $A \in \mathbb{R}^{N \times |S|}$, where N is the number of DSNs. To enhance robustness against noise, we apply a threshold to discard assignments with very small weights.

4.3 DSN State Update

Observation Embedding As described in Section 3, traffic observations X include traffic measurements over a window of time ($X_{traffic}$), static context such as road semantics (X_{static}), and dynamic context such as weather measurements during the same window ($X_{dynamic}$). Embedding these into a fixed-length space captures intra-series correlations efficiently. This also eliminates the need for separate

graph instances for each timestamp, thereby saving memory and computation time.

To embed observations, we first generate the dynamic context $H_{dynamic}$ by processing the time-dependent features $X_{dynamic}$ through a GRU:

$$H_{dynamic} = GRU(X_{dynamic}) \in \mathbb{R}^{|S| \times d_d} \quad (2)$$

We then concatenate $H_{dynamic}$ with static features X_{static} and pass it through an MLP to obtain the context embedding $H_{context}$:

$$H_{context} = MLP([H_{dynamic}; X_{static}]) \in \mathbb{R}^{|S| \times d_c} \quad (3)$$

The traffic sequence $X_{traffic}$ is similarly embedded using a GRU, and the result $H_{traffic}$ is combined with $H_{context}$ to produce the final observation embedding H_{obs} :

$$H_{traffic} = GRU(X_{traffic}) \in \mathbb{R}^{|S| \times d_t} \quad (4)$$

$$H_{obs} = MLP([H_{traffic}; H_{context}]) \in \mathbb{R}^{|S| \times d_e} \quad (5)$$

Here, d_d , d_c , d_t , and d_e are the output dimensions of the GRU and MLP layers.

Observation Aggregation and State Update In this step, we aggregate observation embeddings into the DSN representations they are relevant to. For each DSN $z_i \in Z$, let $A_i \in \mathbb{R}^{|S|}$ denote the i -th row of the thresholded assignment matrix A , which defines the assignment weights from sensors to this DSN. We first scale the observation embeddings H_{obs} by these assignment weights:

$$H_i = A_i H_{obs} \in \mathbb{R}^{|S| \times d_e} \quad (6)$$

This scaling step introduces non-linearity due to the thresholding on A . Next, we aggregate the scaled observation embeddings in H_i to update the state of z_i . After evaluating various aggregation functions (e.g., mean, max, transformers, multi-head attention), we found that the mean function offered the best balance of performance and simplicity. Thus, the update for DSN z_i is:

$$\Delta z_i = \frac{1}{|S_i|} \sum_{s_j \in S_i} H_{i,j} \quad (7)$$

where $S_i = \{s_k \in S \mid A_{i,k} > 0\}$ is the set of sensors with non-zero assignment scores to z_i , and $H_{i,j}$ is their corresponding scaled observation embedding in H_i . Finally, the DSN states Z are updated using a residual connection:

$$Z \leftarrow Z + \Delta Z \quad (8)$$

Long-Short Laplacian After enriching DSN states with traffic observations, it is essential to capture correlations between DSNs to leverage information from related sensors. For example, if a neighborhood experiences rainy weather, the DSN for that neighborhood should be strongly connected to the DSN representing sensors in similar rainy conditions. These correlations are represented as edges in the DSG and are modeled using two types of similarities:

- **Dynamic Short-Term Dependencies** (L_s): This matrix is derived from multi-head attention applied to the updated DSN states Z , capturing short-term dependencies among DSNs within the current time window:

$$L_s = \text{Multihead_Attention}(\text{keys} = Z, \text{queries} = Z) \quad (9)$$

- **Static Long-Term Similarities** (L_l): This matrix captures long-term relationships between DSNs by learning source and target embeddings E_s and E_t for each node across the entire dataset, where $E_s, E_t \in \mathbb{R}^{N \times e}$ and e is the embedding dimension. The long-term similarities are then computed as the softmax of the dot product between node embeddings in E_s and E_t :

$$L_l = \text{softmax}(\text{relu}(E_s \times E_t^T)) \quad (10)$$

The final Laplacian matrix L , termed the Long-Short Laplacian, combines these two matrices as follows:

$$L = \alpha L_s + (1 - \alpha) L_l \quad (11)$$

where α is a learnable parameter. This allows the model to balance short-term and long-term dependencies based on the downstream task. Finally, to enhance sparsity and reduce noise, the smallest $K\%$ of elements in L are pruned.

4.4 DSG Embedding

With the updated DSN states Z and adjacency matrix L , we form the DSG $G = (Z, L)$ for the given observation window. This graph is then processed through a modified Graph Convolutional Network (GCN) (Kipf and Welling 2017), which omits normalization and includes residual connections to preserve directed relationships and mitigate over-smoothing (Chen and et al. 2020). The output is the node embeddings $Z' \in \mathbb{R}^{N \times k}$ (k is the embedding dimension).

Post-convolution, DSN states capture latent traffic information at the sensors within their coverage. To summarize the traffic state across the road network, we apply hierarchical pooling: first, a mixed mean-max-pooling for each DSN type, followed by another pooling to generate a final vector representation $g \in \mathbb{R}^{2k}$ for the entire DSG.

The states Z , Z' , and g represent the traffic state at each DSN, the enriched state considering related DSNs, and the overall state across the network, respectively. We use them for forecasting/reconstruction at query sensor locations.

Table 1: Summary of the time span, sample count, and average number of sensors per sample for each dataset split for both dataset variants: “freeways-only” and “all-roads.”

| Dataset | Time Window | freeways-only | | all-roads | |
|------------|----------------|---------------|---------|-----------|---------|
| | | Samples | Sensors | Samples | Sensors |
| Training | 17.11-29.11.22 | 628 | 4671 | 3714 | 210 |
| Validation | 29.11-06.12.22 | 157 | 4511 | 928 | 193 |
| Test | 06.12-16.12.22 | 339 | 4008 | 1319 | 207 |

4.5 Traffic Inference

In this step, we infer the traffic measurements for the given query set Q . A query $q \in Q$ includes all the non-traffic observation features described in Section 3. To infer the traffic for this query, we first use the assignment functions described in Section 4.2 to find an assignment $A_q \in \mathbb{R}^{1 \times N}$ from this query to the DSN states. Next, we concatenate the query q , the weighted DSNs prior to convolution ($A_q Z$) for DSN-specific context, the weighted embedding of DSNs after convolution which is enriched with related DSNs’ information ($A_q Z'$), and the global DSG embedding (g) for a global view of the traffic network. The global embedding captures additional information that cannot be passed through the local embeddings. This could be an event happening on a different type of road close to the query that might not be well represented solely through the local embedding. This multi-view embedding allows for a comprehensive representation to infer the traffic measurements. We then pass this representation to an MLP to perform the forecasting or reconstruction in a single shot for all the horizon timestamps:

$$\hat{Y}_{traffic} = \text{MLP}([q; A_q Z; A_q Z'; g]) \in \mathbb{R}^{|Q| \times H \times 2} \quad (12)$$

5 Experimental Evaluation

5.1 Experimental Setup

METR-LA+ Dataset Traditional traffic benchmark datasets, such as METR-LA and PEMS-BAY, are constrained by their focus on a limited number of freeway sensors with curated data, where all sensors have uninterrupted observations across all timestamps. To more accurately capture real-world traffic conditions, we introduce **METR-LA+**². METR-LA+ broadens sensor coverage beyond its predecessors by including both freeway and arterial road sensors, while also offering contextual sensor data. To preserve the dataset’s real-world characteristics, no preprocessing was applied to address missing data, thereby retaining the natural occurrence of sensor outages. Further details can be found in Appendix A.

Dataset Configuration We assess two scenarios using METR-LA+: the “freeways-only” scenario, which includes only freeway data, and the default “all-roads” scenario. Each sample in the dataset comprises a 12-timestamp input window, with each timestamp representing a 5-minute interval, covering a total of 1 hour of data. To ensure fair performance

²Due to anonymity, the link is omitted in this version but will be provided in the final paper.

evaluation, we include only samples with at least 1,000 valid sensor recordings per timestamp. Details on the dataset splits are provided in Table 1. For baseline models, missing sensor data is filled with zeros.

Evaluation Setup For each sample, 90% of the sensors are selected as observation sensors, which include both traffic measurements and contextual data in the input window. The remaining 10% are designated as query sensors, providing only contextual data in the input window. We evaluate all baseline models and our approach on traffic reconstruction and forecasting over a horizon of 12 timestamps (60 minutes)³, as discussed in Section 3. Performance is measured using established error metrics: Mean Absolute Error (MAE), Root Mean Squared Error (RMSE), and Mean Absolute Percentage Error (MAPE). Details on hardware, software specifications, and hyperparameters can be found in Appendices B and C.

Baselines We compare our approach against several state-of-the-art time-series forecasting baselines. For fixed sensor graphs, we use DCRNN (Li et al. 2018) and A3tGCN (Bai et al. 2021). Additionally, we include BysGNN (Hajisafi et al. 2023), which combines a fixed sensor graph with meta-nodes that describe the state of similar nodes. For non-sensor graph baselines, we utilize SUSTeR (Wölker et al. 2023). Details on these baselines can be found in Section 2.

Training To train DeepStateGNN, we utilize two training objectives aimed at reducing overfitting and guiding the model to learn effective embeddings for DSNs. The training objectives are as follows:

- **Query Inference Loss (L_1):** This is our primary objective, which minimizes the mean squared error (MSE) of normalized and combined traffic measurements (speed and flow) for each query sensor.
- **Observation Reconstruction Loss (L_2):** This secondary objective regularizes model training by encouraging the model to learn robust Deep State Node embeddings. After constructing the Deep State Graph, we use the observations as queries and attempt to reconstruct their traffic features (which are already available in the input) with minimal error, by minimizing the reconstruction error through MSE.

We combine these objectives and train the model using the final training objective L as follows:

$$L = L_1 + 0.9^\pi * \gamma L_2 \quad (13)$$

where γ is a hyperparameter and π is the current epoch number. This approach assigns greater weight to L_2 at the beginning of training to enhance embedding learning.

5.2 Performance Evaluation

Table 2 presents the performance results of DeepStateGNN and baseline models for traffic reconstruction and forecasting tasks on the METR-LA+ dataset. Our proposed DeepStateGNN consistently outperforms the baselines across all

³Experiments with horizons of 6 timestamps (30 minutes) and 3 timestamps (15 minutes) showed consistent relative performance, so we report results for the 60-minute horizon only.

settings, with the exception of MAPE for traffic flow forecasting and reconstruction in the “all-roads” scenario. Notably, DeepStateGNN achieves up to 40% improvement in traffic flow and 16% in traffic speed for forecasting and reconstruction metrics, respectively. These results highlight the effectiveness of our DeepState Graph representation, which groups similar sensors based on contextual factors to accurately reconstruct or forecast traffic at unknown sensor locations from sparse observations.

A key observation is that the performance improvement is more significant in traffic forecasting than in traffic reconstruction for the same metrics. This difference can be attributed to the difficulty of the forecasting task, which requires predicting future values without knowing any of the prior traffic observations, whereas reconstruction estimates values for the current time window for which some observations are available. This suggests that DeepStateGNN is particularly well-suited for more complex scenarios, leveraging its high-level representation of traffic states for similar sensors.

Among the baselines, DCRNN performs best in the “freeways-only” scenario, consistent with its success in well-known benchmarks like METR-LA and PEMS-BAY. DCRNN’s use of a sensor graph based on road-network distance effectively captures spatial relationships critical to understanding traffic on highways, where signal propagation is strong (Pan et al. 2022). However, in the “all-roads” scenario, while DCRNN remains the best among the baselines (but outperformed by DeepStateGNN) for traffic speed forecasting and reconstruction, A3TGCN (for MAE and RMSE) and SUSTeR (for MAPE) outperform DCRNN in traffic flow forecasting and reconstruction. A3TGCN’s attention-based mechanism and SUSTeR’s abstract nodes allow these models to better capture the diverse patterns seen on arterial roads, where traffic does not necessarily follow the spatial propagation typical of highways.

To further explore the limitations of sensor-graph-based approaches, we compared DeepStateGNN with DCRNN as the ratio of query sensors increased. Initially, 10% of sensors at each timestamp were used as queries, with the remaining sensors serving as observations. In the reconstruction task, as the query ratio increased to 80% and 90%, DCRNN’s MAE for the speed feature increases by 7% and 12%, respectively, and by 21% and 87% for traffic flow. In contrast, DeepStateGNN limited the error increase to less than 3% for speed and 18% for traffic flow. This demonstrates the robustness of DeepStateGNN, which, unlike DCRNN, is not constrained by a sensor-graph, enabling it to effectively handle varying amounts of missing sensors.

5.3 Computation Time

To assess the scalability of DeepStateGNN, we compare its training time per epoch with that of baseline models using our “all-roads” dataset. For this analysis, we limit the number of sensors to subsets of 200, 1000, 3000, and 4000. Each experiment is repeated three times on an identical GPU with a batch size of 32.

Figure 2 presents the training time results. DeepStateGNN shows the fastest training times for larger sen-

Table 2: Performance comparison between DeepStateGNN and baseline models for traffic forecasting and reconstruction tasks across the “freeways-only” and “all-roads” dataset scenarios. Results are reported as the mean \pm standard deviation over 3 runs. The lowest error in each setup is highlighted in **bold**, while the second-best error is *underlined*. The “Improvement” row indicates the percentage improvement of DeepStateGNN over the next best baseline for each metric and task.

| Baseline | Metric | freeways-only | | | | all-roads | | | |
|----------------|--------|------------------------------------|--------------------------------------|------------------------------------|--------------------------------------|------------------------------------|-------------------------------------|------------------------------------|-------------------------------------|
| | | Reconstruction | | Forecast | | Reconstruction | | Forecast | |
| | | Speed | Flow | Speed | Flow | Speed | Flow | Speed | Flow |
| A3TGCN | RMSE | 11.77 \pm 0.06 | 5.82 \pm 0.21 | 12.02 \pm 0.23 | 6.01 \pm 0.33 | 8.48 \pm 0.04 | <u>5.21 \pm 0.00</u> | 9.16 \pm 0.02 | <u>5.91 \pm 0.11</u> |
| | MAE | 8.66 \pm 0.15 | 3.82 \pm 0.41 | 9.02 \pm 0.28 | 4.19 \pm 0.47 | 5.05 \pm 0.14 | <u>2.59 \pm 0.01</u> | 5.59 \pm 0.10 | <u>3.26 \pm 0.24</u> |
| | MAPE | 23.41 \pm 0.96 | 142.32 \pm 47.38 | 24.13 \pm 2.01 | 166.38 \pm 50.40 | 26.30 \pm 1.11 | 113.06 \pm 4.78 | 27.93 \pm 0.18 | 142.75 \pm 23.04 |
| BysGNN | RMSE | 11.55 \pm 0.27 | 6.20 \pm 0.25 | 12.04 \pm 0.64 | 6.03 \pm 0.30 | 7.01 \pm 0.02 | 6.41 \pm 0.60 | 7.66 \pm 0.22 | 6.71 \pm 0.27 |
| | MAE | 8.31 \pm 0.23 | 4.15 \pm 0.24 | 8.65 \pm 0.08 | 3.94 \pm 0.11 | 4.58 \pm 0.22 | 4.57 \pm 0.71 | 4.69 \pm 0.03 | 4.76 \pm 0.38 |
| | RMSE | 22.47 \pm 1.98 | 189.29 \pm 6.78 | 24.58 \pm 1.40 | 162.60 \pm 36.51 | 25.63 \pm 0.88 | 179.89 \pm 44.82 | 25.60 \pm 0.18 | 196.20 \pm 18.29 |
| DCRNN | RMSE | <u>9.64 \pm 0.68</u> | <u>4.88 \pm 0.58</u> | <u>10.95 \pm 0.70</u> | <u>5.47 \pm 0.57</u> | <u>5.70 \pm 0.09</u> | 5.59 \pm 0.51 | <u>6.10 \pm 0.28</u> | 6.25 \pm 0.39 |
| | MAE | <u>6.74 \pm 0.66</u> | <u>2.90 \pm 0.66</u> | <u>7.82 \pm 0.64</u> | <u>3.58 \pm 0.61</u> | <u>3.94 \pm 0.44</u> | 3.03 \pm 0.97 | <u>4.23 \pm 0.56</u> | 3.83 \pm 0.93 |
| | MAPE | <u>17.56 \pm 1.67</u> | <u>107.22 \pm 44.74</u> | <u>20.89 \pm 2.50</u> | <u>142.74 \pm 41.17</u> | <u>23.47 \pm 0.01</u> | 140.81 \pm 60.56 | <u>24.55 \pm 0.46</u> | 165.50 \pm 68.44 |
| SUSTeR | RMSE | 12.49 \pm 0.05 | 6.83 \pm 0.05 | 12.65 \pm 0.10 | 6.80 \pm 0.17 | 9.01 \pm 0.04 | 5.83 \pm 0.05 | 9.62 \pm 0.02 | 6.17 \pm 0.08 |
| | MAE | 8.81 \pm 0.00 | 4.61 \pm 0.01 | 8.91 \pm 0.01 | 4.61 \pm 0.10 | 4.88 \pm 0.02 | 3.31 \pm 0.03 | 5.18 \pm 0.01 | 3.52 \pm 0.07 |
| | MAPE | 26.35 \pm 0.43 | 230.72 \pm 2.09 | 26.68 \pm 0.63 | 221.00 \pm 8.01 | 26.42 \pm 0.17 | 92.30 \pm 0.45 | 27.05 \pm 0.04 | 105.85 \pm 1.04 |
| DeepStateGNN | RMSE | 8.47 \pm 0.06 | 4.06 \pm 0.04 | 9.20 \pm 0.19 | 4.35 \pm 0.10 | 5.21 \pm 0.00 | 4.89 \pm 0.01 | 5.55 \pm 0.01 | 5.52 \pm 0.02 |
| | MAE | 5.94 \pm 0.08 | 2.34 \pm 0.04 | 6.37 \pm 0.14 | 2.56 \pm 0.12 | 3.48 \pm 0.01 | 2.38 \pm 0.03 | 3.70 \pm 0.02 | 2.96 \pm 0.05 |
| | MAPE | 15.12 \pm 0.26 | 79.03 \pm 5.30 | 17.00 \pm 0.16 | 84.85 \pm 12.26 | 21.36 \pm 0.04 | <u>104.44 \pm 2.40</u> | 22.09 \pm 0.08 | <u>112.54 \pm 4.69</u> |
| Improvement(%) | RMSE | 12.14% | 16.80% | 15.98% | 20.48% | 8.60% | 6.14% | 9.02% | 6.60% |
| | MAE | 11.87% | 19.31% | 18.54% | 28.49% | 11.68% | 8.11% | 12.53% | 9.20% |
| | MAPE | 13.90% | 26.29% | 18.62% | 40.56% | 8.99% | * | 10.02% | * |

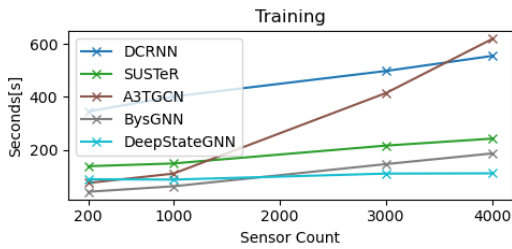


Figure 2: Training time per epoch with a constant batch size.

sensor sets. For smaller datasets, the fixed size of the DeepStateGNN graph is similar to the sensor graph in other models, causing DeepStateGNN to perform less efficiently. However, as the sensor count increases, DeepStateGNN demonstrates significant scalability advantages, maintaining a linear scaling pattern with a much slower growth rate than all other baselines, approaching near-constant behavior. This highlights DeepStateGNN’s efficiency in handling larger datasets compared to other models.

5.4 Ablation Study

To evaluate the contributions of different components in DeepStateGNN, we compare the full model (DSG) against four variants: removing dynamic DSNs (DSG_{-d}), static DSNs (DSG_{-s}), message passing (DSG_{-gcn}), and observation reconstruction loss (DSG_{-L2}). Table 3 reports error metrics for average speed reconstruction on the “all-roads” scenario. The full model outperforms the ablated variants in 9 out of 12 metric comparisons, with only minor differences observed in favor of DSG_{-d} for MAPE (0.03% lower), DSG_{-gcn} for RMSE (0.01 lower), and a tie in MAE with DSG_{-d} . This underscores the importance of incorporating

Table 3: Ablation study: Speed reconstruction on the “all-roads” scenario. Metrics represent the mean values of 3 runs, with standard deviation omitted due to negligible variation.

| Metric | DSG | DSG_{-d} | DSG_{-s} | DSG_{-gcn} | DSG_{-L2} |
|--------|--------|------------|------------|--------------|-------------|
| MAE | 5.21 | 5.21 | 5.37 | 5.24 | 8.9 |
| RMSE | 3.48 | 3.51 | 3.72 | 3.47 | 4.9 |
| MAPE | 21.36% | 21.33% | 22.28% | 21.45% | 25.9% |

both static and dynamic DSNs and leveraging message passing for sensor group correlations.

While DSG_{-d} shows only a slight performance decline, the configuration using only dynamic DSNs (DSG_{-s}) still significantly outperforms the best baseline (DCRNN) on the same task, indicating dynamic context like weather is important but that spatial features like neighborhood have a greater impact. The DSG_{-L2} variant sees a notable 70% drop in MAE, emphasizing the critical role of observation reconstruction loss in regularizing model training and improving generalization.

6 Conclusion

In this work, we presented DeepStateGNN, a novel GNN framework that clusters traffic sensors into high-level nodes based on contextual similarity and observed patterns, forming a fixed-size DeepState graph. This approach addresses key limitations in previous GNN-based traffic forecasting methods, particularly in terms of scalability, flexibility, and effectiveness in handling incomplete traffic observations. Our extensive experiments on the new METR-LA+ dataset demonstrated that DeepStateGNN significantly outperforms state-of-the-art baselines in both traffic forecasting and reconstruction tasks, while also offering improved computational efficiency.

References

- Bai, J.; Zhu, J.; Song, Y.; Zhao, L.; Hou, Z.; Du, R.; and Li, H. 2021. A3T-GCN: Attention Temporal Graph Convolutional Network for Traffic Forecasting. *ISPRS International Journal of Geo-Information*, 10(7).
- Chen, D.; and et al. 2020. Measuring and relieving the over-smoothing problem for graph neural networks from the topological view. In *AAAI*, volume 34, 3438–3445.
- Hajisafi, A.; Lin, H.; Shaham, S.; Hu, H.; Siampou, M. D.; Chiang, Y.-Y.; and Shahabi, C. 2023. Learning Dynamic Graphs from All Contextual Information for Accurate Point-of-Interest Visit Forecasting. In *Proceedings of the 31st ACM International Conference on Advances in Geographic Information Systems, SIGSPATIAL '23*. New York, NY, USA: Association for Computing Machinery. ISBN 9798400701689.
- Kipf, T. N.; and Welling, M. 2017. Semi-Supervised Classification with Graph Convolutional Networks. In *ICLR*.
- Li, L.; Jiang, R.; He, Z.; Chen, X. M.; and Zhou, X. 2020. Trajectory data-based traffic flow studies: A revisit. *Transportation Research Part C: Emerging Technologies*, 114: 225–240.
- Li, Y.; Yu, R.; Shahabi, C.; and Liu, Y. 2018. Diffusion Convolutional Recurrent Neural Network: Data-Driven Traffic Forecasting. In *International Conference on Learning Representations (ICLR '18)*.
- Pan, Z.; Zhang, W.; Liang, Y.; Zhang, W.; Yu, Y.; Zhang, J.; and Zheng, Y. 2022. Spatio-Temporal Meta Learning for Urban Traffic Prediction. *IEEE Transactions on Knowledge and Data Engineering*, 34(3): 1462–1476.
- Shao, Z.; Zhang, Z.; Wei, W.; Wang, F.; Xu, Y.; Cao, X.; and Jensen, C. S. 2022. Decoupled Dynamic Spatial-Temporal Graph Neural Network for Traffic Forecasting. *Proc. VLDB Endow.*, 15(11): 2733–2746.
- Veličković, P.; Cucurull, G.; Casanova, A.; Romero, A.; Liò, P.; and Bengio, Y. 2018. Graph Attention Networks. In *International Conference on Learning Representations*.
- Wölker, Y.; Beth, C.; Renz, M.; and Biastoch, A. 2023. SUSTeR: Sparse Unstructured Spatio Temporal Reconstruction on Traffic Prediction. *SIGSPATIAL '23*. New York, NY, USA: Association for Computing Machinery. ISBN 9798400701689.
- Wu, Z.; Pan, S.; Long, G.; Jiang, J.; and Zhang, C. 2019. Graph wavenet for deep spatial-temporal graph modeling. In *Proceedings of the 28th International Joint Conference on Artificial Intelligence, IJCAI'19*, 1907–1913. AAAI Press. ISBN 9780999241141.
- Yu, B.; Yin, H.; and Zhu, Z. 2018. Spatio-temporal graph convolutional networks: a deep learning framework for traffic forecasting. In *Proceedings of the 27th International Joint Conference on Artificial Intelligence, IJCAI'18*, 3634–3640. AAAI Press. ISBN 9780999241127.